Biochimica et Biophysica Acta, 943 (1988) 331–342
Elsevier

BBA 74088

Thermotropic lipid phase separation in the human immunodeficiency virus

Larry M. Gordon [a], Fred C. Jensen [b], Cyril C. Curtain [c], Patrick W. Mobley [d] and Roland C. Aloia [e]

[a] *Rees-Stealy Research Foundation, San Diego, CA,* [b] *Cytotech, San Diego, CA (U.S.A.),* [c] *CSIRO, Division of Biotechnology, Clayton (Australia),* [d] *Chemistry Department, California State Polytechnic University, Pomona, CA, and* [e] *Anesthesiology Service, J.L. Pettis Memorial V.A. Hospital, Loma Linda, CA and Departments of Anesthesiology and Biochemistry, Loma Linda University School of Medicine, Loma Linda, CA (U.S.A.)*

(Received 22 December 1987)

Key words: HIV; AIDS; Lipid domain; Cholesterol; Membrane fluidity; ESR; Spin probe

The presence of thermodependent lipid domains in the envelope of the human immunodeficiency virus (HIV) was studied. HIV was propagated in Hut-78 cells and purified by differential-gradient centrifugation. Since the virus was highly infectious in cell culture and Western blots of detergent-inactivated HIV showed envelope proteins when exposed to sera containing anti-HIV antibodies, this viral preparation was not deficient in 'spike' or 'knob' particles. Electron spin resonance (ESR) studies of intact HIV labeled with 5-nitroxide stearate (5-NS) indicated that a temperature-dependent lipid phase separation occurs with a high onset at approx. 42°C and a low onset at approx. 15°C. Cooling below 42°C induces 5-NS clustering. Similar phase separations with high onsets at approx. 37–38°C were previously identified in 5-NS labeled human erythrocytes (cholesterol/phospholipid (C/P) molar ratio = 0.90) and cholesterol-loaded (C/P = 0.85–0.98) rat liver plasma membranes. These were attributed to a temperature-sensitive redistribution of endogenous lipid components such that 5-NS is excluded from cholesterol-rich domains and tends to reside in cholesterol-poor domains at low temperatures. Since HIV has a lipid envelope with a similarly high C/P of 0.88 (Aloia et al. (1988) Proc. Natl. Acad. Sci. USA 85, 900–904), cholesterol-rich and cholesterol-poor domains also probably exist in HIV at physiologic temperatures. The reduced stability and infectivity of HIV noted on heating above 42°C may be due, in part, to the abolition of these thermodependent domains.

Introduction

The budding and release of enveloped viruses from the surface of infected cells is an exquisite example of domain formation in biological membranes. With type-C retroviruses, the viral envelope consists of: (i) lipids derived from the host-cell plasma membrane; and (ii) hydrophobic 'spike' proteins intercalated into the lipid matrix

Abbreviations: HIV, human immunodeficiency virus; AIDS, acquired immunodeficiency syndrome; ARC, AIDS-related Complex; ELISA, enzyme-linked immunosorbent assay; 5-NS, the *N*-oxyl-4′,4′-dimethyloxazolidine derivative of 5′-ketostearic acid; P/L, the ratio of probe molecules to total lipid (phospholipid + cholesterol) molecules; C/P, cholesterol/phospholipid molar ratio; gp41, glycoprotein 41 (the 'spike', or transmembrane portion of the envelope protein); gp120, glycoprotein 120 (the 'knob', or exposed portion of the envelope protein); p17, p20, p23, p24, p27, p31, p34, p39, p51, p55 and p66, HIV-encoded proteins; L, liquid lipid domains; S, solid lipid domains; QCC, quasicrystalline cluster lipid domains; S, polarity-corrected order parameter; $S(T_{\parallel})$, polarity-uncorrected order parameter; $S(T_{\perp})$, polarity-uncorrected order parameter; AL 721, cholesterol-poor liposome; DPH, 1,6-diphenylhexatriene.

Correspondence: L.M. Gordon, Rees-Stealy Research Foundation, San Diego, CA 92101, U.S.A. and R.C. Aloia, Anesthesiology Service, J.L. Pettis V.A. Hospital, Loma Linda, CA 92357, U.S.A.

that are covalently linked to hydrophilic 'knob' glycoproteins. The timely production of mature virions from the host cell presents the retrovirus with a considerable architectural problem. On the one hand, viral-encoded coat proteins must be transported from endoplasmic reticulum and assembled in localized patches in the cell surface. On the other hand, native proteins in the host plasma membranes must be quantitatively excluded from the maturing viral envelope. The mechanism(s) by which viruses achieve this lateral domain formation and compartmentation prior to release is unclear, but may involve the sequestration of specific membrane lipids. For example, several workers have reported that the cholesterol content of enveloped viruses may exceed by as much as 2-fold that of the host-plasma membrane [1,2]. This agrees with the general finding that animal viruses have high molar ratios (about 1) of cholesterol/phospholipid if the virion is assembled at the cell surface [3].

Here we consider the related problem of whether discrete lipid domains exist within the envelope of purified HIV. It is a matter of some interest to define the topological distribution of lipids in HIV, particularly since this virus is responsible for the AIDS pandemic. Similar to other retroviruses, electron microscopy indicates that the envelope of HIV is contiguous with the plasma membrane of the lymphocyte surface from which the virus buds [4,5]. This suggests that the HIV coat proteins recruit native lymphocyte lipids to form the viral envelope. Earlier, we reported that the C/P molar ratio of the HIV envelope is high [6], analogous to that of other animal viruses [3] and such biological membranes as human red blood cells and rat liver plasma membranes [7,8]. Since previous spin-label studies of native and cholesterol-loaded rat liver plasma membranes and human red blood cells showed the presence of thermodependent cholesterol-rich and cholesterol-poor domains [7–9], this ESR methodology is used here to assign the existence of similar domains in the HIV envelope.

Materials and Methods

5-Nitroxide stearate (5-NS) was purchased from Aldrich Chemical Co. (St. Louis, MO) and thin-layer chromatographic analysis demonstrated negligible impurities [10].

Purified virus was obtained from HIV-producing OKT-4$^+$ leukemic cells (Hut-78), as described earlier [6]. High levels of HIV infectivity were determined by incubating H-9 cells with virus [6]. For protein and lipid analyses and ESR experiments, pelleted virus was resuspended at 9 mg protein/ml in 137 mM NaCl/15 mM Na_2HPO_4/1.5 mM KH_2PO_4/2.7 mM KCl/0.5 mM $MgCl_2$ (pH 7.5). Protein, phospholipid and cholesterol contents were measured as in Ref. 6.

Three isolates of HIV were used: (i) LK013 from the peripheral blood lymphocytes of a male homosexual who subsequently died of AIDS (December, 1985); (ii) COO1SE from the ejaculate of the above male homosexual; and (iii) F7529 from the lymph nodes of a female sex partner (i.e., ARC patient) of an intravenous drug abuser.

To test for viral-specific proteins in these HIV preparations, Western blots were performed. Purified HIV was disrupted by 1% Triton X-100 and 0.1% deoxycholate and boiled for 5 min. The HIV proteins were resolved by SDS-polyacrylamide gel electrophoresis (5–6 h at 35 mA). The separated proteins were transblotted onto 0.22 μm nitrocellulose (16 h at 5–10 mA and at 100 mA for 1 h). The nitrocellulose was washed in phosphate buffered saline and blocked with 5% 'blotto' for 2 h at 37°C. The nitrocellulose was cut into 2-mm strips, and individual strips were reacted with a 1:100 dilution of test serum overnight at 4°C. After washing, bound antibodies were reacted with goat anti-human IgG labeled with horseradish peroxidase. After incubating for 1 h at 37°C, unbound antibodies were washed and a substrate containing 4-chloro-1-naphthol and hydrogen peroxide was added at room temperature.

For electron microscopy, thin-sections of HIV-producing Hut-78 cells were stained with uranyl acetate and lead citrate and photographed with a Zeiss 109 electron microscope.

All spin-labeling of HIV was performed in a biosafety level 3 facility, with approval from the National Cancer Institute. 5-NS was dissolved in ethanol ($3 \cdot 10^{-2}$ M) and aliquots were dried with a stream of dry N_2 gas in plastic vials. HIV samples (15 μl aliquots) were added to the probe and hand-vortexed for several minutes, at room

temperature. Spin-labeled HIV (7 μl aliquots) were drawn into 50 μl capillary pipettes, that were subsequently heat-sealed at both ends. The sealed capillaries were inspected with a light microscope (40 × magnification), and then inserted into a special holder (attributed to R. Kornberg [11]) and fabricated out of Kel-F by John Markel (J & M Specialities, San Diego, CA). The Kornberg holder containing spin-labeled HIV was carefully introduced into the Dewar of the variable temperature regulator of the EPR spectrometer. Before turning on the nitrogen gas flow, polypropylene tubing was fitted over the top of the Dewar and led to a suction flask containing 5 M NaOH (i.e., a base concentration that rapidly inactivates HIV). Since the nitrogen gas was vented through the NaOH solution, any sudden change in gas pressure, loosening of the Kornberg holder or breaking of the heat-sealed capillary would not expose the atmosphere to aerosols of 'live' HIV. The extent of 5-NS incorporation was tested by comparing the amount of probe added to the viral suspension (i.e., μg 5-NS/mg protein 'weight') with the paramagnetic spins observed in the microwave cavity (i.e., μg 5-NS/mg protein 'spins'). Spins were calculated from the ratio of the double-integrated spectrum of 5-NS-labeled HIV with that of the Varian strongpitch (0.1% pitch, with $3 \cdot 10^{15}$ spins in 5.5 mm [12–14]).

ESR spectra were recorded with a Varian E-109 spectrometer fitted with a Deltron (Sydney) Model DCM 20 temperature control accessory [6,15], digitized with a Hewlett-Packard 7470A plotter and 9816 computer, and stored on floppy discs [12,13].

The following order parameters may be used to assess the flexibility of the fatty-acid spin probe:

$$S(T_\parallel) = 1/2\left[\frac{3(T_\parallel - 6.1)}{26.3} - 1\right] \quad (1)$$

$$S(T_\perp) = 1/2\left[\frac{3[38.5 - 2T_\perp]}{26.3} - 1\right] \quad (2)$$

$$S = 0.5653[(T_\parallel - T_\perp)/(1/3T_\parallel + 2/3T_\perp)] \quad (3)$$

where $T_\parallel$ and $T_\perp$ (see Fig. 1) for the HIV-incorporated probe are the hyperfine splitting elements parallel and perpendicular to z', the symmetry axis of the effective Hamiltonian (H'). S, $S(T_\parallel)$ and $S(T_\perp)$ are sensitive to membrane fluidity (or, more accurately, the flexibility of the incorporated probe). These order parameters may assume values between 0 and 1, with the extremes indicating that the probe samples respectively fluid and immobilized environments. S, which requires both splittings, corrects for small polarity differences between the membrane and reference crystal [10,16].

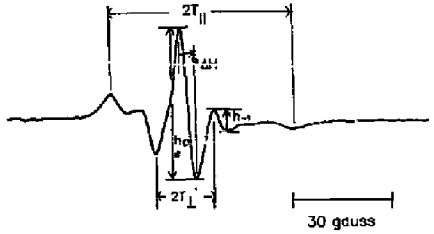

Fig. 1. Electron spin resonance (ESR) spectrum of intact HIV labeled with 5-nitroxide stearate (5-NS) at 37 °C. Spectra were recorded as described in the text. The horizontal axis represents varying magnetic field, while the vertical axis reflects absorption of microwaves. Instrument conditions were: 8 min scan time, 3.2 G modulation amplitude, 10 mW microwave power, and 1 s time constant. Outer and inner hyperfine splittings, $2T_\parallel$ and $2T_\perp$, were measured as shown; $2T_\perp$ was corrected by the addition of 1.6 G [10]. The peak-to-peak distance of the central line (ΔH) is indicated. Respective heights of the central line (h_0) and the highfield peak of the inner hyperfine doublet (h_{-1}) are shown. The μg probe/mg protein and P/L ratios, determined from the number of spins in the spectrum, were 1.03 and 1/139, respectively [12].

Probe–probe interactions were estimated using three empirical parameters [10,14,17,18]. The first involves measuring the peak-to-peak width of the central line (i.e., ΔH of Fig. 1).

$$\Delta H = \Delta H_0 + \Delta H_{dip} + \Delta H_{ex} \quad (4)$$

where ΔH_0 is the linewidth without interactions, ΔH_{dip} is the line broadening caused by magnetic dipolar interactions, and ΔH_{ex} is contributed by spin–spin exchange [10]. Enhanced probe–probe interactions increase ΔH. The second measure is based on the observation that $S(T_\perp)$, but not $S(T_\parallel)$, decreases with P/L in various membranes, including HIV [10,12–14]. Thus, with $\Delta S(T_\parallel)$ remaining zero, decreases in $S(T_\perp)$ (i.e., $\Delta S(T_\perp) < 0$) indicate greater probe–probe interactions. The third parameter depends on the height of the

high-field peak of the inner hyperfine doublet (h_{-1} in Fig. 1), decreasing with respect to that of the central line (h_0): h_{-1}/h_0 declines as the probe concentration is elevated [10,12–14].

Results

HIV morphogenesis and morphology

Electron microscopy shows that HIV 'buds' from the surface of host lymphocytes following membrane insertion of virus-encoded glycoproteins [4,5]. Hence, the plasma membrane is used as a 'template' to produce viral particles. Consistent with the view that this retrovirus is derived from the lymphocyte surface membrane is our earlier finding of a high cholesterol/phospholipid (C/P) molar ratio of 0.88 for HIV [6]. The lymphocyte plasma membrane, with the highest C/P ratio of all the membrane organelles [19], is the probable source of HIV lipids. Mature virions released during this budding process are clearly seen in Fig. 2. Viral particles are spherical with dense cylindrical cores, which appear either round or bar shaped in the electron micrograph depending on the sectioning plane. The fuzzy surface of HIV particles is due to glycoprotein spikes in the envelope. Mature virions are notably pleomorphic, with spherical diameters ranging from 110 to 130 nm (Fig. 2).

Presence of 'spike' and 'knob' glycoproteins in the envelope of HIV

Since HIV *env* proteins may be lost during extraction procedures [20], one may question whether our differentially centrifuged preparations contain gp120 and gp41. That this is not a problem is suggested by the high infectivity of cell culture by these viral isolates; infection of OKT4$^+$ lymphocytes requires a full complement of *env* proteins. Moreover, the isolates were used to prepare Western blots of sera containing anti-HIV antibodies (Fig. 3), and showed gp120 and gp41 bands, besides other HIV-encoded proteins.

Fluidity of HIV spin-labeled with 5-nitroxide stearate (5-NS)

The dynamic, or 'fluid', properties of the lipids of HIV were studied by incorporating spin probes into the envelope of intact virions. With HIV (9 mg protein/ml) at 37°C, the ESR spectrum in Fig. 1 shows that 5-NS readily inserts into the membrane, since no probe partitions into the aqueous buffer. In agreement with our previous

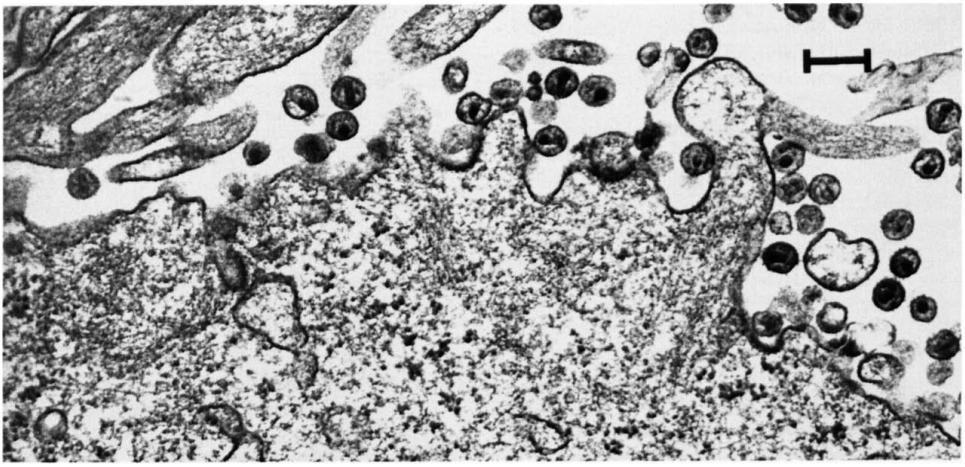

Fig. 2. Electron micrograph of HIV (F7529 isolate) budding from cultured Hut-78 lymphocytes. Mature virions with well-defined cores are seen at the cell periphery. Bar equals 200 nm.

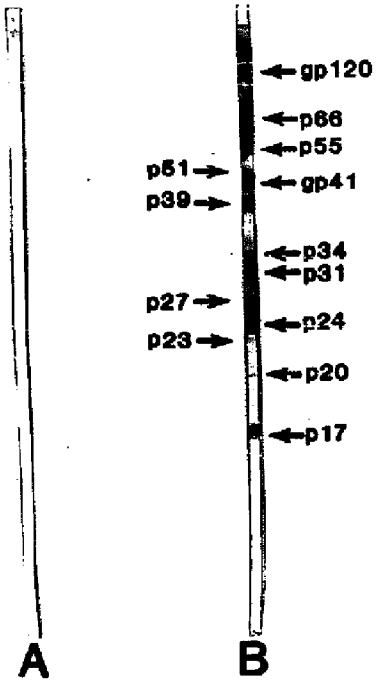

Fig. 3. Western blots of detergent-disrupted HIV (F7529). (A) Serum from a healthy control, seronegative for anti-HIV antibodies on ELISA; (B) serum from an asymptomatic patient, seropositive for anti-HIV antibodies on ELISA. Bands for the 'spike' (gp41) and 'knob' (gp120) proteins are shown, as well as other HIV-encoded proteins (p17, p20, p23, p24, p31, p34, p39, p51, p55 and p66).

studies [6], the spectrum indicates that 5-NS rapidly rotates about its long molecular axis (about 10^8 revolutions/s), with movement away from the preferred orientation severely restricted. This rapid anisotropic motion creates an effective symmetry axis. $2T_{\parallel}$ and $2T_{\perp}$ are the hyperfine splittings due to the interaction of the spin of the unpaired electron with the nuclear spin of the ^{14}N and are measured from the ESR spectra parallel and perpendicular to the unique symmetry axis (Fig. 1). Increases in $2T_{\parallel}$ and decreases in $2T_{\perp}$ signal a decreased mobility of the oxazolidine reporter group.

Spin probe clustering and its' effect on the ESR spectra and order parameters of 5-NS labeled HIV

An important question in spin-label studies of HIV concerns whether probe–probe interaction effects interfere with the measurement of 'intrinsic' membrane properties [17]. Here, 'intrinsic' properties are defined as those which are measured when probe interactions are negligible, and do not refer to membrane behavior in the absence of a perturbing label. To assess this problem with HIV, intact virions were labeled with a wide range of 5-NS probe concentrations as described previously [14,17]. For μg probe/mg protein 'wt' ratios of 1 to 18, HIV shows only a limited capacity for 5-NS uptake (Fig. 4). Progressively decreased additional incorporation occurred at higher loading. Incomplete probe uptake at high loading was confirmed by noting 5-NS remaining as a deposit on the side of the tube.

It is of some interest to contrast the % uptake of 5-NS into HIV in Fig. 4 with the corresponding curve for human red blood cell ghosts. Similar to the findings with HIV, red blood cell ghosts show only a restricted ability to solubilize 5-NS (Fig. 4). Our interpretation of the red cell results is that 5-NS binds at specific membrane sites. Previous Scatchard analysis indicated that 5-NS interaction with ghosts cannot be viewed as a simple partitioning phenomenon of an infinitely dilute solute

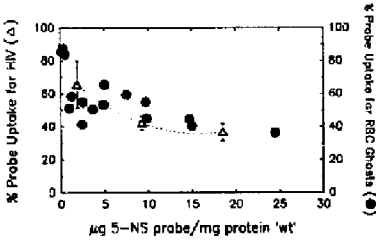

Fig. 4. Plot of % probe uptake vs. weight of 5-NS probe added to 15 μl aliquots of HIV (9 mg protein/ml) (△·····△) or 50 μl of human red blood cell ghosts (12 mg protein/ml) (●) [12]. % Probe uptake was calculated from the ratio of the probe weight added to the sample (i.e., μg probe/mg protein 'wt') to that determined from the spins in the spectra (i.e., μg probe/mg protein 'spins'). HIV values are means ± 1S.D. for at least three determinations. The higher S.D. at low loading may be due to the saturation of 'high-affinity' sites over a narrow probe concentration range.

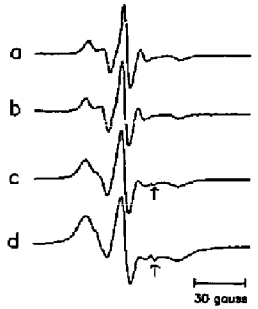

Fig. 5. ESR spectra of HIV (9 mg protein/ml at 37°C) labeled with varying concentrations of 5-NS. Lipid/probe (μg probe/mg protein 'spins') ratios were: (a) 139 (1.03); (b) 86 (1.66); (c) 35 (4.10); and (d) 21 (6.80). The liquid lines indicated by arrows in (c) and (d) are due to 5-NS tumbling in aqueous solution.

in an ideal solvent (see Fig. 2B of Ref. 12). For low levels of bound probe, 5-NS binds to a single class of sites with high affinity. However, the 5-NS binding isotherm exhibits such significant curvature at high loading that further probe uptake by ghosts is reduced. Although one explanation for these results is that 5-NS binds to two classes of independent sites, it is more likely that, once occupied, the probe-membrane sites act through a cooperative mechanism to inhibit additional 5-NS binding (see below and Ref. 12). The similar behavior for the HIV curve in Fig. 4 argues that an analogous model may also account for 5-NS interactions with the viral envelope.

Since μg probe/mg protein 'wt' does not accurately indicate probe insertion, all probe/lipid (P/L) or μg probe/mg protein ratios used in the following experiments were assessed from the paramagnetic spins of the spectrum.

To assess 5-NS concentration effects on the ESR spectra of HIV, spectra were recorded with P/L ranging from 1/139 to 1/21 (Fig. 5). At a P/L of 1/139, the spectrum indicates that the probe undergoes rapid anisotropic motion about its long molecular axis at 37°C (Fig. 5a). Raising the P/L from 1/139 to 1/21 decreased h_{-1} with respect to h_0, displaced downward the high-field baseline and upward the low-field baseline, increased $2T_\perp$ and ΔH and left $2T_\parallel$ unchanged (Fig. 5c, d). Similar probe-dependent spectral alterations have been reported with a variety of biological membranes, including human erythrocytes (for review, see Refs. 12, 17).

The above 5-NS probe titrations exerted profound effects on HIV order parameters and empirical parameters sensitive to radical interactions. Increasing the 5-NS/lipid up to 1/86 did not affect S, $S(T_\parallel)$ or $S(T_\perp)$ (Fig. 6). Raising the probe concentration above this 'low' P/L range, however, decreased substantially S and $S(T_\perp)$, while $S(T_\parallel)$ was relatively constant. These order parameter effects are most likely due to enhanced radical interactions and not membrane fluidization. The broadening of $T_\perp$ (and decrease in $S(T_\perp)$) was closely correlated with increases in ΔH (Fig. 6); prior investigations have demonstrated that radical interactions broaden the ΔH of labeled model and biological membranes [10,17]. Reductions in S and $S(T_\perp)$ were also associated with such characteristic exchange-broadening effects as the decrease in the high-field peak of the inner hyperfine doublet (h_{-1} in Fig. 1) and the downward displacement of the high-field baseline (Fig. 5c, d). The finding that $T_\parallel$ (or $S(T_\parallel)$) is essentially unaltered for HIV in this P/L range indicates that the 'apparent' increase in fluidity with probe concentration, denoted by reductions in S and $S(T_\perp)$, is not due to probe-mediated perturbations; any fluidization allowing more probe flexibility requires that $T_\parallel$ narrow commensurately with increases in $2T_\perp$ and h_{-1}, and that ΔH decreases.

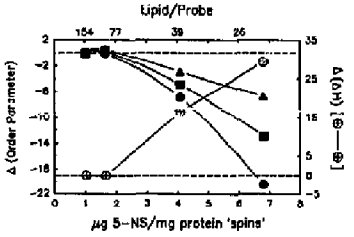

Fig. 6. Effects of 5-nitroxide stearate concentration on the order parameters and ΔH of intact HIV at 37°C. $\Delta S(T_\parallel)$ (▲), $\Delta S(T_\perp)$ (●) and ΔS (■) are percent changes from baseline values measured at a P/L of 1/139. Control $S(T_\parallel)$, $S(T_\perp)$ and S were 0.731, 0.595 and 0.651. $\Delta(\Delta H)$ (⊕) is the percent change in ΔH from the baseline value of 4.20 G.

Comparable 5-NS concentration effects on order parameters and ΔH have been noted in many other biological membranes (for review, see Refs. 10, 12). In previous studies on 5-NS labeled erythrocyte ghosts (Fig. 4 of Ref. 12), these parameters depended similarly on probe concentration. It is unlikely that the above probe effects are the result of enhanced probe–probe interactions due to dipolar broadening, but are instead a consequence of augmented spin-exchange interactions. This is because the probe executes rapid anisotropic motion at 37°C and dipole–dipole interactions are relatively long-range, tending to be averaged out by rapid diffusion and/or tumbling, while exchange interactions require that labels be in van der Waal's contact and decrease rapidly with distance.

There are several conclusions from the above probe titration experiments. First, Fig. 6 shows that the order parameters of HIV reflect 'intrinsic' membrane properties, for 'low' 5-NS/lipid ratios, approx. 1/100. With this low probe/lipid at 37°C, excellent agreement was seen in the polarity-corrected order parameters obtained from HIV isolates LK013 ($S = 0.651$), COO1SE ($S = 0.651$) and F7529 ($S = 0.652$) at 37°C [6]. As we have previously shown [6,12], the high S for HIV is similar to that of human erythrocyte ghosts ($S = 0.640$). Both HIV and red cells have rigid membranes at physiologic temperature, possibly due to the high C/P of 0.88 and 0.90, respectively [6,9]. Furthermore, either $S(T_\perp)$ or ΔH may be used to empirically estimate probe–probe interactions in HIV labeled with 'high' P/L – more than approx. 1/86.

It is worthwhile to consider the structural basis for enhanced nitroxide radical interactions in the envelope of HIV. Recently, we have developed a cluster model for 5-NS distribution in human erythrocyte ghosts that accurately simulates ESR spectral alterations observed with increasing P/L at 37°C [12,13]. This probe occupies a class of high-affinity, noninteracting sites at low loading. Saturation occurs with increasing probe concentration, and at higher loading, the probe inserts itself at initially dilute sites to form membrane-bound clusters of variable size. No magnetically-dilute probe remains at the 'very high' P/L range, where all 5-NS clusters in a concentrated phase. The above model allows determination of the dilute/clustered ratio for any given P/L ratio, and validates our earlier use of empirical parameters sensitive to radical interactions (i.e., ΔH or $\Delta S(T_\perp)$) in estimating probe sequestration in biological membranes [10,17]. The alternative model that spin-exchange arises from rapid lateral diffusion of uniformly distributed 5-NS is rejected because probe uptake cannot be regarded as a partitioning phenomenon of an infinitely-dilute solute in an ideal solvent. Since the reduced uptake of additional probe occurs at the same P/L where spectral broadening is manifest (Fig. 4) [12,13], an important initial condition for stimulating spectra via the lateral diffusion model and modified Bloch equations [21] has been invalidated. The similar actions of increasing 5-NS/lipid on the ESR spectra (Fig. 5), probe uptake (Fig. 4), order parameters and ΔH (Fig. 6) of HIV suggest that this cluster model is also applicable to the 5-NS labeled viral envelope. Namely, that the enhanced probe interactions in 5-NS labeled HIV at high loading are due to probe clustering.

Thermotropic lipid phase separation in 5-NS labeled HIV

The presence of a temperature-dependent (i.e., thermotropic) lipid phase separation in the HIV envelope was assessed with a spin-label methodology previously used to assign thermodependent lipid domains in other high-cholesterol biomembranes [7,8,18]. Temperature-dependent ESR spectra were recorded for HIV labeled with a concentration of 5-NS that is in the low-range at 37°C (Fig. 7). Above 37°C, the ESR spectra show that the 5-NS probe executes rapid anisotropic motion about its long molecular axis, with more limited fatty acyl-chain flexing away from this axis. Cooling below 37°C dramatically alters the ESR spectra, with progressive increases in the outer splitting ($2T_\parallel$) and ΔH, and decreases in the inner splitting ($2T_\perp$). Below about 10°C, the high-field peak of the inner hyperfine doublet becomes poorly resolved due to slow probe motion.

The effects of temperature changes on the flexibility of the 5-NS probe in HIV may be quantitated by calculating $S(T_\parallel)$ from the ESR spectra of Fig. 7. An Arrhenius plot of the $S(T_\parallel)$ from

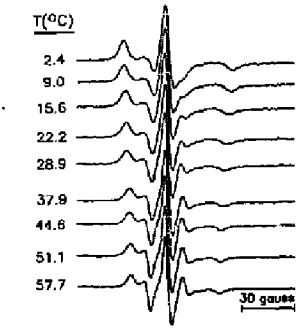

Fig. 7. Temperature-dependent ESR spectra of HIV labeled with a concentration of 5-nitroxide stearate that is in the 'low' range at 37°C. (LK013 isolate; labeled with μg probe/mg protein or P/L ratios of 1.03 or 1/139). Spectra were recorded from low to high temperatures, with 4 min waits for equilibration at each temperature.

HIV labeled with a low 5-NS/lipid ratio demonstrated progressive increases in probe flexibility with increasing temperature (2–60°C) (Fig. 8). Furthermore, this plot indicated a minor 'break' or 'discontinuity' at about 15°C, suggestive of a broad lipid phase separation with an onset at about 15°C that perturbs 5-NS flexibility. Examination of this Arrhenius plot did not, however, readily indicate whether this onset was the low- or high-temperature end of a thermotropic lipid phase separation.

To further investigate the nature of this lipid phase separation, thermodependent ESR spectra were recorded with HIV labeled with a 5-NS concentration that is in the 'high' range at 37°C (Fig. 9). Raising the temperature over a wide range (2–60°C) altered the ESR spectra of HIV labeled with 'high' range 5-NS in a manner qualitatively similar to results obtained with a 'low' 5-NS concentration (Fig. 7). Above 37°C, the ESR spectra show that the 5-NS probe executes rapid anisotropic motion about its long molecular axis, with restricted fatty acyl-chain flexing away from the axis. Besides this probe flexibility, however, comparison with 'low' range ESR spectra for temperatures above 37°C (Fig. 7) indicates that probe–probe interactions occur in 'high' range

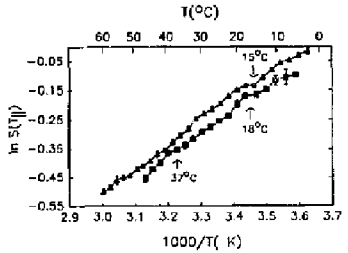

Fig. 8. Arrhenius plots of $S(T_{\parallel})$ for 5-NS-labeled HIV (▲) or cholesterol-enriched rat liver plasma membranes (■). $S(T_{\parallel})$ was calculated from Eqn. 1 for intact HIV virions loaded with 1.0 μg 5-NS/mg protein. HIV results are means ± S.D. for three separate preparations (one of the LK013 isolate and two of the COO1SE isolate); the absence of an error bar indicates that the S.D. is less than the symbol size. The presence of a minor 'break' or 'discontinuity' at about 15°C in the HIV plot indicates the onset of a thermotropic lipid phase separation (see text). For rat liver plasma membranes artifically enriched with cholesterol [22], $S(T_{\parallel})$ was calculated for membranes labeled with 6 μg 5-NS/mg protein. Results are means ± 1 S.D. for three preparations, with C/P of 0.98, 0.97 and 0.94; the absence of an error bar indicates the S.D. is less than the symbol size. 'Breaks' or 'discontinuities' at 37°C and 18°C reflect the high and low onsets of a broad thermotropic lipid phase separation in high-cholesterol rat liver plasma membranes (see Ref. 8).

ESR spectra (Fig. 9), probably due to enhanced spin-exchange interactions of clustered probe (see above). Cooling below 37°C markedly changed

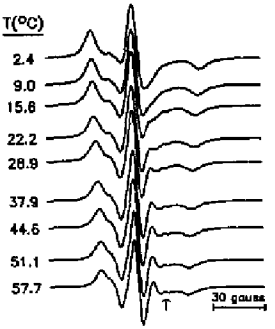

Fig. 9. Temperature-dependent ESR spectra of HIV labeled with a concentration of 5-NS that is in the 'high' range at 37°C. (LK013 isolate; labeled with μg probe/mg protein or P/L ratios of 4.10 or 1/35.) The arrow indicates a 'liquid-line' component due to the 5-NS probe tumbling in the aqueous buffer.

the ESR spectra, with progressive increases in the outer splitting ($2T_{\parallel}$) and decreases in the inner splitting ($2T_{\perp}$) until about 22°C, where the high-field peak of the inner hyperfine double becomes poorly resolved due to slow probe motion and enhanced probe–probe interactions. It is of some interest to note that, for each temperature in Figs. 7 and 9, the $2T_{\parallel}$ values are similar for 'low' and 'high' probe concentrations, while the 'high'-range $2T_{\perp}$ splittings become increasingly larger than the corresponding 'low'-range values at the lower temperatures (Figs. 7, 9). Since $2T_{\perp}$ is an empirical parameter sensitive to probe–probe interactions when $\Delta T_{\parallel} \approx 0$ (see above and Refs. 12, 13, 18), the qualitative impression is that probe–probe interactions substantially increase as spin-labeled HIV is cooled below 37°C. Enhanced probe–probe interactions in the 'high' range spectra at low temperatures probably account for the loss of the high-field peak of the inner hyperfine splitting doublet (i.e., h_{-1} in Fig. 1) at much higher temperatures (i.e., about 10°C for 'low'-range spectra (Fig. 7) and about 20°C for 'high'-range spectra (Fig. 9)).

It is worthwhile contrasting the actions of temperature change on the order parameters of HIV labeled with 'low' and 'high' 5-NS concentrations. For HIV labeled with a 'low' probe concentration, Arrhenius-type plots of S, $S(T_{\parallel})$ and $S(T_{\perp})$ (Fig. 10A) show that temperature reductions increase each order parameter. Fig. 10A also indicates that the slopes of the 'low'-range order parameter vs. $1/T$ (K) curves becomes steeper in the following order: $S(T_{\perp}) < S < S(T_{\parallel})$. Effects of temperature on the order parameters were also examined with HIV labeled with a high 5-NS concentration (Fig. 10A). The $S(T_{\parallel})$ vs. $1/T$ (K) curves using either 'low' or 'high' probe concentrations were in good agreement throughout the temperature range 2–60°C. However, 'high'-range S and $S(T_{\perp})$ values were considerably less than corresponding 'low'-range order parameters for each temperature in the range 42–20°C. It should be noted that S and $S(T_{\perp})$ values could not be determined for 'low'- and 'high'-range spectra for temperatures below about 10 and 20°C, respectively, due to poorly resolved hyperfine splittings (Figs. 7, 9).

The thermodependence of probe–probe interactions in 5-NS labeled HIV was quantitatively evaluated from difference order parameter vs. $1/T$ (K) plots, calculated as the percent difference between values obtained at 'high' and 'low' probe concentrations. Fig. 10B demonstrates that $\Delta S(T_{\perp})$ and ΔS become increasingly more negative below about 42°C, while $\Delta S(T_{\parallel})$ does not significantly vary from zero. The invariance of $S(T_{\parallel})$ suggests that, for 'low' and 'high' probe concentrations, ESR spectra reflect only those 5-NS that sample lipid domains sharing the same fluidity and polarity. Since it is reasonable to assume that the flexibility and polarity contributions to 'low'- and 'high'-range $S(T_{\parallel})$ will be equal at a given temperature [10], $\Delta S(T_{\perp})$ (or, alternatively, $\Delta T_{\perp}$) is here an empirical parameter

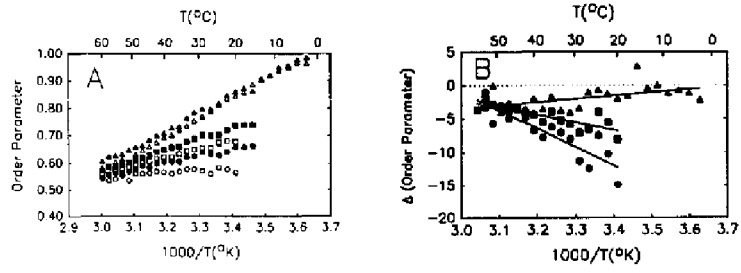

Fig. 10. Temperature-dependence of the order parameters of 5-NS labeled HIV (LK013 isolate). (A) $S(T_{\parallel})$ (▲), S (■) and $S(T_{\perp})$ (●) were measured using a 'low' probe concentration (i.e., 1.03 μg probe/mg protein), while $S(T_{\parallel})$ (△), S (□) and $S(T_{\perp})$ (○) were obtained with a 'high' probe concentration (i.e., 4.10 μg probe/mg protein). (B) Δ(order parameter) were the percent differences between values measured at the 'high' and 'low' probe concentrations of (A), for $S(T_{\parallel})$ (▲), S (■) and $S(T_{\perp})$ (●).

reflecting only radical interactions. It should be recalled that $S(T_\perp)$ decreased as the 5-NS concentration increased in HIV at 37°C, while $S(T_\parallel)$ remained essentially unchanged (Fig. 6). The observation that $\Delta S(T_\perp)$ becomes more negative below 42°C suggests that cooling also promotes probe–probe interactions in the HIV envelope. For reasons discussed with other 5-NS labeled membranes [7,8], the progressively enhanced probe–probe interactions which occurred as 5-NS labeled HIV was cooled below 42°C are attributed to enhanced spin–exchange interactions due to greater probe clustering.

The following thermotropic lipid phase separation model is proposed to account for the above ESR results on 5-NS labeled HIV. Temperature-sensitive lipid domains occur in the envelope of HIV with high and low onsets of 42 and 15°C. As the HIV envelope is cooled below 42°C, the 5-NS probe progressively segregates, and this probe clustering is mediated by a lateral redistribution of native lipid components. The low onset of the phase separation perturbs 5-NS flexibility, and is probably responsible for the loss of rapid anisotropic motion seen at approx. 15°C (Fig. 7).

Discussion

It is of interest to contrast the putative thermotropic lipid phase separation in HIV with those identified in native ($C/P = 0.71$) and cholesterol-enriched ($C/P = 0.85$–0.98) rat liver plasma membranes [7,8,22] and human erythrocyte ghosts [8]. Using native rat liver plasma membranes labeled with a low 5-NS concentration, Arrhenius-type plots of order parameters demonstrated 'breaks' at 28 and 19°C, suggesting low and high onsets for a broad lipid phase separation that perturb 5-NS flexibility [7,17]. Furthermore, Arrhenius-type plots of Δ(order parameters) indicated 5-NS segregation below 28°C [7,9,18]. For reasons discussed earlier [18], we proposed a model for native rat liver plasma membranes in which solid (S) and liquid (L) lipid domains coexist below 19°C. The 19°C break corresponds to S and L dispersed into 'quasicrystalline' clusters (QCC) and L. Here, QCC are defined as having a packing density and fluidity between that of S and L. QCC decrease with heating above 19°C until the 28°C transition is reached and remaining QCC are converted into L. Thus, the enhanced 5-NS clustering in Δ(order parameter) vs. $1/T$ (K) plots of native membranes below 28°C [7] suggests that the formation of probe-excluding QCC tends to segregate 5-NS in L.

The nature of the thermotropic lipid phase separation in rat liver plasma membranes was further examined through artificial loading to high C/P molar ratios [22]. For cholesterol-enriched ($C/P = 0.85$–0.98) liver plasma membranes labeled with a 'low' 5-NS concentration, an Arrhenius plot of $S(T_\parallel)$ indicated 'breaks' at approx. 37°C and 18°C (Fig. 8) [8]. This suggests that cholesterol loading raises the high onset of the broad lipid phase separation from 28°C to 37°C, while leaving the low onset at approx. 19°C unaffected. Consistent with this hypothesis is the finding that cholesterol enrichment elevates the onset temperature at which 5-NS clusters from 28°C to 37–38°C [7–9]. The most likely explanation of these data is that the QCC and L of native rat liver plasma membranes are cholesterol-rich domains and -poor domains, respectively, and that cholesterol enrichment increases the proportion of QCC to L at physiologic temperatures.

The broad lipid phase separation (42–15°C) identified in the HIV envelope ($C/P = 0.88$) is likely to be similar to that of both cholesterol-enriched ($C/P = 0.85$ to 0.98) rat liver plasma membranes (37–18°C) and human erythrocyte ghosts [7,8]. The Arrhenius plot of the $S(T_\parallel)$ of HIV may be superimposed with that of high-cholesterol liver membranes, simply by shifting the HIV curve to the right by approx. 3 C° (Fig. 8). Moreover, Arrhenius-type plots of Δ(order parameter) indicate that HIV and cholesterol-enriched liver membranes segregate 5-NS below 42°C and 37–38°C, respectively (Fig. 10) [7,8]. Given the similar C/P ratios of human erythrocyte ghosts ($C/P = 0.90$) and the HIV envelope ($C/P = 0.88$) [6], it is also of interest that 5-NS labeled erythrocyte ghosts show a thermotropic lipid phase separation, probably involving the formation of cholesterol-rich and -poor lipid domains [8]. The temperature onsets of the phase separation in erythrocytes closely match those of HIV and high-cholesterol liver membranes [8].

An important consideration in interpreting the above ESR results centers on whether the 5-NS probe binds nonspecifically to viral proteins. If a substantial fraction of the 5-NS probe were to interact with HIV proteins, then the above phase-separation model would be rendered moot. For the following reasons, however, our initial studies indicate that 5-NS principally binds to envelope lipid. Although the spectrum of 5-NS labeled HIV reflects an ordered membrane environment, there is no evidence in Figs. 1 and 7 of a second, immobilized component characteristic of probe bound to envelope proteins (gp120 or gp41) or core proteins (p17 or p24). The view that 5-NS principally samples the lipid envelope was supported by our ability to accurately simulate these spectra with computer programs, assuming that the spin probe resides in a homogeneous region (Curtain et al., unpublished observations). Last, previous experiments on 5-NS labeled HIV and human erythrocyte ghosts showed identical ESR spectra, order parameters and probe polarity at 37°C (see Fig. 2B in Ref. 6). Since the C/P ratios and phospholipid compositions of HIV and erythrocyte ghosts are identical [6], while the respective protein compositions are widely different, the simplest explanation for the interchangeable spectra is that 5-NS samples similar lipid environments in both membranes. Nevertheless, the above discussion does not exclude the possibility that a small proportion of the 5-NS probe (e.g., less than 5–10%) nonspecifically interacts with HIV envelope proteins. In future ESR studies, it will be of much interest to examine 5-NS labeled lipid extracts of HIV to more quantitative assess the role (if any) that proteins play in probe binding.

After submission of this manuscript, an article appeared confirming certain aspects of the results presented here [23]. Similar to findings with HIV isolates LK013, F7529 and COO1SE [6], Crews et al. [23] reported that other strains of HIV have high C/P ratios ($C/P > 1.0$) and rigid envelops, as indicated by the fluorescent probe DPH. Moreover, an Arrhenius plot of the fluorescence polarization of DPH-labeled HIV over the range 40–4°C showed a change of slope at about 21°C [23]. This 'break' probably corresponds to the low-temperature onset of the lipid phase separation identified above with 5-NS. Interestingly, extraction of cholesterol by treating HIV with AL-721 dramatically fluidized the viral envelope and eliminated the 21°C break [23]. Since high cholesterol levels typically suppress phase transitions in model phospholipid mixtures [24], it is unlikely that the low-temperature break in native HIV is due to a classical gel → liquid lipid melt. If such were the case, removal of cholesterol would be expected to enhance the transition rather than abolishing it, as Crews et al. [23] observed. Instead, a more plausible explanation is that the low-temperature break is due to a lateral redistribution of cholesterol, as predicted by the above phase-separation model.

The presence of cholesterol-rich domains in the HIV envelope may play an important role in maintaining viral infectivity at physiologic temperatures. HIV is stable for long periods at 37°C, but is rapidly inactivated above 42°C [25,26], with the virus losing infectivity by a logarithmic factor of 3 after 1 h at 56°C. Since the temperature at which HIV becomes unstable coincides with the high onset of the proposed phase separation, it is tempting to speculate that the formation of cholesterol-rich domains is protective. Earlier rat liver plasma membrane studies [7,8,22] showed that cholesterol enrichment concurrently increased the amount of cholesterol-rich QCC and protected adenylate cyclase from thermal denaturation.

Acknowledgments

We gratefully acknowledge technical assistance from Virginia Lee and Dan Ripley (Cytotech, Inc., San Diego, CA), graphics from the Audio-Visual Department (J.L. Pettis VA Hospital, Loma Linda, CA), Mrs. Marilyn Woodward (Departments of Pathology and Electron Microscopy, Sharp Hospital, San Diego, CA) for electron microscopy, and the administration of the J.L. Pettis VA Hospital for construction of a biosafety level 3 laboratory. We thank Drs. H.-Y. Cheung and R.D. Sauerheber for reading the article, Drs. Robin and Luibel for the use of their electron microscopy facilities (Sharp Hospital, San Diego, CA), and Drs. F. Crews and A. Lippa for providing a preprint of their article. We appreciate financial support from the Texas Academy for the

Advancement of Life Sciences and Mr. and Mrs. Al Gordon.

References

1 Renkonen, O., Kaarainen, L., Simmons, K. and Gahmberg, C. (1971) Virology 46, 318–326.
2 Slosberg, B.N. and Montelaro, R.C. (1982) Biochim. Biophys Acta 689, 393–402.
3 Blough, H.A. and Tiffany, J.M. (1972) Adv. Lipid Res. 10, 267–339.
4 Montagnier, L. (1986) Prog. Allerg. 37, 46–64.
5 Gallo, R.C., Samgadharan, M.G., Popovic, M., Shaw, G.M., Hahn, B., Wong-Staal, F., Robert-Guroff, M., Salahuddin, S.Z. and Markham, P.D. (1986) Prog. Allerg. 37, 1–45.
6 Aloia, R.C., Jensen, F.C., Curtain, C.C., Mobley, P.W. and Gordon, L.M. (1988) Proc. Natl. Acad. Sci. U.S.A. 85, 900–904.
7 Gordon, L.M., Mobley, P.W., Esgate, J., Hofmann, G., Whetton, A.D. and Houslay, M.D. (1983) J. Membrane Biol. 76, 139–149.
8 Gordon, L.M. and Mobley, P.W. (1984) J. Membrane Biol. 79, 75–86.
9 Gordon, L.M. and Mobley, P.W. (1985) in Membrane Fluidity in Biology (Aloia, R.C. and Boggs, J., eds.), Vol. 4, pp. 1–49, Academic Press, New York.
10 Curtain, C.C. and Gordon, L.M. (1984) in Membranes, Detergents and Receptor Solubilization (Venter, J.C. and Harrison, L., eds.), Vol. 1, pp. 177–213, Alan R. Liss, New York.
11 Gaffney, B.J. (1974) Methods Enzymol. 32B, 151–198.
12 Gordon, L.M., Looney, F.D. and Curtain, C.C. (1985) J. Membrane Biol. 84, 81–95.
13 Gordon, L.M., Looney, F.D. and Curtain, C.C. (1987) Biochim. Biophys. Acta 898, 202–213.
14 Curtain, C.C., Looney, F.D. and Gordon, L.M. (1987) Methods Enzymol. 150, 418–446.
15 Aloia, R.C., Paxton, J., Daviau, J.S., van Gelb, O., Mlekusch, W., Truppe, W., Meyer, J.A. and Brauer, F.S. (1985) Life Sci. 36, 1003–1017.
16 Gordon, L.M. and Sauerheber, R.D. (1977) Biochim. Biophys. Acta 466, 34–43.
17 Sauerheber, R.D., Gordon, L.M., Crosland, R. and Kuwahara, M. (1977) J. Membrane Biol. 31, 131–169.
18 Gordon, L.M., Sauerheber, R.D. and Esgate, J.A. (1978) J. Supramol. Struct. 9, 299–326.
19 Van Blitterswijk, W.J., Emmelot, P., Hilkmann, H.A.M., Oomen-Meulemans, E.P.M. and Inbar, M. (1977) Biochim. Biophys. Acta 467, 309–320.
20 Laurence, J. (1987) Infect. Med. 4, 187–228.
21 Devaux, P., Scandella, C.J. and McConnell, H.M. (1973) J. Magn. Reson. 9, 474–485.
22 Whetton, A.D., Gordon, L.M. and Houslay, M.D. (1983) Biochem. J. 210, 437–449.
23 Crews, F.T., McElhaney, M.R., Klepner, C.A. and Lippa, A.S. (1988) Drug Development Res., in press.
24 Cossins, A.R. and Sinensky, M. (1984) in Physiology of Membrane Fluidity (Shinitzky, M., ed.), Vol. 2, pp. 1–20, CRC Press, Boca Raton.
25 McDougal, J.S., Martin L.S., Cort, S.P., Mozen, M., Heldebrant, C.M. and Evatt, B.L. (1986) J. Clin. Invest. 76, 875–877.
26 Spire, B., Dormont, D., Barre-Sinoussi, F., Montagnier, L. and Chermann, J.C. (1985) Lancet i, 188–189.